

ROS-mediated vascular homeostatic control of root-to-shoot soil Na delivery in *Arabidopsis*

Caifu Jiang¹, Eric J Belfield¹, Aziz Mithani^{1,2},
Anne Visscher¹, Jiannis Ragoussis³,
Richard Mott³, J Andrew C Smith¹
and Nicholas P Harberd^{1,*}

¹Department of Plant Sciences, University of Oxford, Oxford, UK,

²Department of Biology, Syed Babar Ali School of Science and Engineering, Lahore University of Management Sciences, Sector U, DHA, Lahore, Pakistan and ³The Wellcome Trust Centre for Human Genetics, University of Oxford, Oxford, UK

Sodium (Na) is ubiquitous in soils, and is transported to plant shoots via transpiration through xylem elements in the vascular tissue. However, excess Na is damaging. Accordingly, control of xylem-sap Na concentration is important for maintenance of shoot Na homeostasis, especially under Na stress conditions. Here we report that shoot Na homeostasis of *Arabidopsis thaliana* plants grown in saline soils is conferred by reactive oxygen species (ROS) regulation of xylem-sap Na concentrations. We show that lack of *A. thaliana* respiratory burst oxidase protein F (AtrbohF; an NADPH oxidase catalysing ROS production) causes hypersensitivity of shoots to soil salinity. Lack of AtrbohF-dependent salinity-induced vascular ROS accumulation leads to increased Na concentrations in root vasculature cells and in xylem sap, thus causing delivery of damaging amounts of Na to the shoot. We also show that the excess shoot Na delivery caused by lack of AtrbohF is dependent upon transpiration. We conclude that AtrbohF increases ROS levels in wild-type root vasculature in response to raised soil salinity, thereby limiting Na concentrations in xylem sap, and in turn protecting shoot cells from transpiration-dependent delivery of excess Na.

The EMBO Journal (2012) 31, 4359–4370. doi:10.1038/emboj.2012.273; Published online 12 October 2012

Subject Categories: plant biology

Keywords: *Arabidopsis*; Na homeostasis; NADPH oxidase; ROS; salt tolerance

Introduction

Soil salinity is one of the major factors limiting global agricultural production, affecting an estimated ~20 million hectares of cultivated land world-wide (Epstein, 1985; Zhu, 2002; Flowers, 2004; Munns and Tester, 2008). In addition, increased salinisation of cultivated land, especially where production depends on irrigation, is threatening the sustainability of global food production (Greenway and Munns, 1980; Frommer *et al.*, 1999; Tester and Davenport,

2003; Flowers, 2004; Munns and Tester, 2008). Thus, there is an urgent need to advance the understanding of plant soil-salinity tolerance mechanisms, and to increase the salinity tolerance of crops.

Soil salinity is characterized by a high concentration of soluble salts. NaCl is the most soluble and widespread soil salt, and Na⁺ toxicity is therefore the most prevalent natural salinity stress restricting plant growth (Zhu, 2002; Tester and Davenport, 2003; Munns and Tester, 2008). Many plants have evolved mechanisms to circumvent the effects of high soil Na⁺ concentrations, including maintenance of shoot and root intracellular Na⁺ concentrations at non-toxic levels (Zhu, 2002; Munns and Tester, 2008). In *Arabidopsis*, delivery of Na⁺ from the soil to shoot is believed to involve the following steps. Initially, Na⁺ enters root epidermal cells passively via nonselective cation channels (Amtmann and Sanders, 1999; Tester and Davenport, 2003; Munns and Tester, 2008) and likely also via high-affinity K⁺ (HKT) transporters (Munns and Tester, 2008). Next, Na⁺ moves across the endodermis, and then enters the cells of the central vascular cylinder (stele). Finally, Na⁺ is loaded from the stelar cells into the xylem elements specialized for long-distance transport (vessels and tracheids), and is thereby delivered to the shoot in the transpiration stream (Smith, 1991; Davenport *et al.*, 2007; Munns and Tester, 2008). Working against this root-to-shoot Na⁺ flow, there are mechanisms that restrict the amount of Na⁺ delivered to the shoot. First, plasma membrane Na⁺/H⁺ antiporters (e.g., SOS1) can pump Na⁺ back into soil solution, reducing the net influx of Na⁺ into inner cell layers of the root (Shi *et al.*, 2002; Zhu, 2002; Munns and Tester, 2008; Quintero *et al.*, 2011). This reverse pumping of Na⁺ into the soil is dependent on additional factors (e.g., SOS2, SOS3 and the putative calcium sensor CBL10; Qiu *et al.*, 2002, 2004; Quan *et al.*, 2007). Second, HKT transporters can retrieve Na⁺ from the transpiration stream in the xylem before it reaches the shoots (Mäser *et al.*, 2002; Ren *et al.*, 2005; Sunarpi *et al.*, 2005; Davenport *et al.*, 2007; Møller *et al.*, 2009; Baxter *et al.*, 2010; Munns *et al.*, 2012). These mechanisms for counteracting root-to-shoot Na⁺ delivery are essential for maintaining shoot Na⁺ concentrations at non-toxic levels and thus for soil-salinity tolerance (Zhu, 2002; Munns and Tester, 2008).

Soil-salinity stress causes the *in planta* accumulation of reactive oxygen species (ROS) (Achard *et al.*, 2008; Miller *et al.*, 2010), which secondarily results in oxidative stress and cell damage (Flowers, 2004; Miller *et al.*, 2010; Xie *et al.*, 2011). In addition, there is evidence suggesting that ROS, as well as being a toxic agent in salinity stress, also acts as a signalling mediator of plant salinity tolerance. For example, *Arabidopsis* mutants lacking cytosolic and/or chloroplastic H₂O₂ ascorbate peroxidase removal enzymes were found to be more tolerant of salinity stress, suggesting that increased ROS levels promote tolerance (Miller *et al.*, 2007). In addition, it has recently been reported that the enzyme At5PTase7 regulates ROS

*Corresponding author. Department of Plant Sciences, University of Oxford, South Parks Road, Oxford OX1 3RB, UK. Tel.: +44 1865 275071; Fax: +44 1865 275074; E-mail: nicholas.harberd@plants.ox.ac.uk

Received: 23 May 2012; accepted: 12 September 2012; published online: 12 October 2012

production in saline conditions (likely through activation of NADPH oxidase enzymes), and that mutants lacking At5PTase7 activity are hypersensitive to salinity (Kaye *et al*, 2011). Finally, treatment of wild-type (WT) *Arabidopsis* plants with diphenylene iodonium (DPI, an inhibitor of NADPH oxidase activity) blocked salinity-induced ROS production and reduced salinity tolerance by inhibiting gp91^{phox} homologues (also called respiratory burst oxidase; Leshem *et al*, 2007). ROS therefore plays a dual role in salinity response, potentially causing oxidative damage as well as conferring salinity tolerance (Dat *et al*, 2000). However, to our knowledge, no ROS-associated genes have previously been identified following forward-genetic screens for mutants with altered salinity sensitivity. In addition, the cellular mechanisms by which *in vivo* ROS production and ROS signalling promote salinity tolerance remain unknown.

Previous genetic screens for *Arabidopsis thaliana* mutants displaying altered salinity responses have largely involved *in vitro* (Petri-dish) environments (Liu *et al*, 2000; Quesad *et al*, 2000; Shi *et al*, 2002), and have enabled the discovery of genes (including *SOS1*, *SOS2* and *SOS3*) playing major roles in plant salinity response and tolerance (Zhu, 2002). However, the relative artificiality of these *in vitro* screens (in particular the limitations on transpiration rate) might have resulted in additional genes important to plant soil-salinity response being missed (Møller and Tester, 2007). We therefore devised a novel screen for *A. thaliana* mutants hypersensitive to soil salinity, with special focus on the possibility that such mutants might be affected in the delivery of Na from root to shoot (see Materials and methods section). We describe here the isolation of a novel soil-salinity hypersensitive mutant from this screen, and show that the mutant phenotype is conferred by a loss-of-function allele of *A. thaliana* respiratory burst oxidase protein *F* (*AtrbohF*), a gene whose product is an NADPH oxidase that catalyses production of ROS. We subsequently show that *AtrbohF* increases root vascular ROS levels in response to soil salinity, thus reducing xylem-sap Na levels and delivery of Na to the shoot, hence protecting the shoot from the damaging effects of excess Na. In addition, we show that delivery of excess Na to the shoot caused by lack of *AtrbohF* is dependent upon a functioning transpiration stream. For the first time, we show how tissue-specific ROS production regulates root–shoot Na delivery and consequent Na tolerance in transpiring soil-grown plants typical of natural and agricultural environments.

Results

Identification of an *A. thaliana* soil-salinity sensitive-1-1 (*sss1-1*) mutant

Our previous work had shown that the abscisic acid (ABA) and ethylene signalling pathways can integrate plant salinity responses via the DELLAs, a family of growth-inhibitory proteins particularly associated with gibberellin signalling (Achard *et al*, 2006). However, DELLA-deficient *A. thaliana* mutants actually display mild salinity sensitivity (Achard *et al*, 2006), thus indicating the relative importance of DELLA-independent salinity responses. We therefore screened for mutants displaying soil-salinity hypersensitivity derived from a DELLA-deficient *A. thaliana* progenitor line (see Materials and methods section). Screening of approximately 50 000 fast

neutron-mutagenised DELLA-deficient M₂ seedlings (see Materials and methods section; Belfield *et al*, 2012) yielded 10 mutants displaying hypersensitivity to soil salinity. Among these, the *sss1-1* mutant phenotype was shown by backcrossing to be conferred by a single recessive allele. *sss1-1* mutants display a characteristic bleaching phenotype 10 days after being watered with 120 mM NaCl, while progenitor controls remain green (Figure 1A). This bleaching is due to a dramatic decrease (~60%) in *sss1-1* chlorophyll content (Figure 1B and C) and associated cell death (Figure 1D). Interestingly, although *sss1-1* is hypersensitive to a range of soil NaCl concentrations (Supplementary Figure 1A and B), there was no detectable difference between the salt sensitivities of *in vitro* grown *sss1-1* and control plants (Supplementary Figure 1C). Thus, *sss1-1* identifies a gene that regulates plant sensitivity to soil but not to *in vitro* salinity.

sss1-1 is a novel mutant *AtrbohF* allele

We identified the mutation conferring *sss1-1* phenotype via whole-genome sequence analysis (see Materials and methods section; Jiang *et al*, 2011; Belfield *et al*, 2012). Of five novel mutations in the *sss1-1* genome (versus the progenitor genome; Supplementary Figure 1D), only one (an 8025-bp inversion; Chr1: 23 765 370–23 773 866) was uniformly homozygous in ~60 soil-salinity hypersensitive F₂ plants obtained following a backcross between *sss1-1* and the progenitor (data not shown). This inversion interrupts gene At1G64060, a gene encoding a gp91^{phox} homologue and previously designated as *AtrbohF* (Figure 2A; Torres *et al*, 2002, 2005).

To confirm that loss of *AtrbohF* function confers the *sss1-1* phenotype, we showed that *atrbohF-F3* (a loss-of-function *AtrbohF* allele derived from the *A. thaliana* Col-0 (WT) genetic background; Torres *et al*, 2002) homozygotes and *sss1-1/atrbohF-F3* heterozygotes both display soil-salinity hypersensitivity (Figure 2B and C). Thus, loss of *AtrbohF* function confers hypersensitivity to soil salinity. In addition, loss of *AtrbohF* function confers soil-salinity hypersensitivity irrespective of the presence or absence of DELLA function.

AtrbohF is expressed in root vascular tissue

We next studied the effect of salinity on *AtrbohF* transcripts. Exposure to salinity caused marginal increases in *AtrbohF* transcript levels 2–6 h following treatment onset, and more substantial increases after 24–72 h (especially in the root; Figure 3A), suggesting that an increase in *AtrbohF* transcript levels might confer enhanced soil-salinity tolerance. We next investigated the cell/tissue specificity of *AtrbohF* expression, using *pAtrbohF::GUS* plants expressing *Escherichia coli* β-glucuronidase (GUS) under the control of an *AtrbohF* promoter fragment (Materials and methods section). GUS activity was predominantly detected in roots of *pAtrbohF::GUS* plants (Figure 3B), mainly in cells comprising the central vascular cylinder or stele (Figure 3C and D). Cross-sectional analysis detected GUS activity primarily within the pericycle cells and associated vascular parenchyma, but not in xylem vessels (Figure 3E and F). In addition, we found that salinity caused a tissue-/cellular-specific increase in GUS staining in root stele cells (Figure 3G–I). These observations indicate that *AtrbohF* is mainly expressed in the root stele, and that salinity increases stele-specific expression of *AtrbohF*.

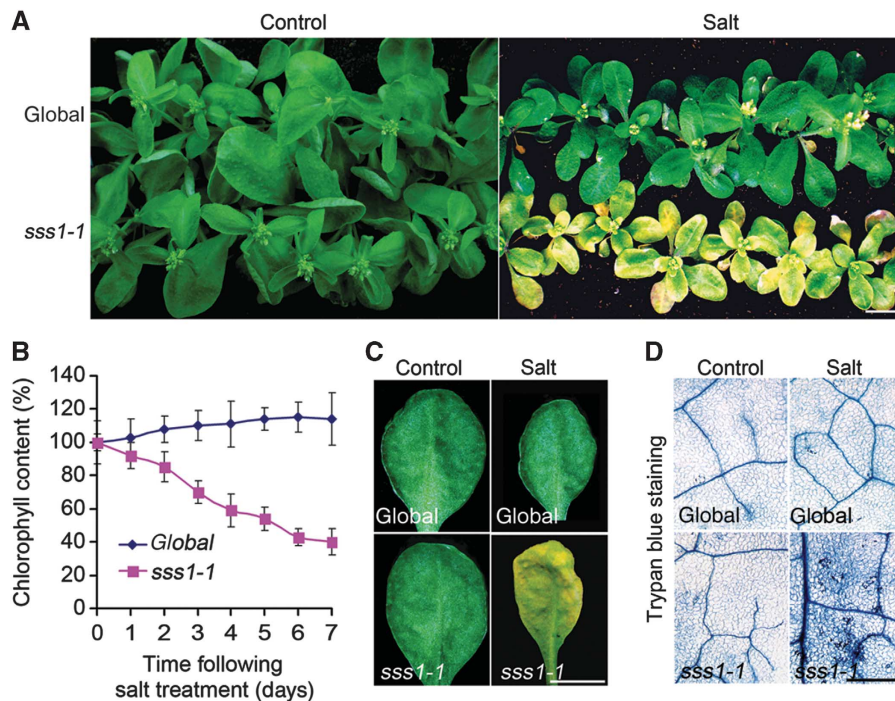


Figure 1 Initial characterization of the *sss1-1* mutant. (A) Mutant (*sss1-1*) and DELLA-deficient progenitor (global) control plants were grown on soil in standard conditions for 4 weeks, then watered once to soil capacity with either 120 mM NaCl (Salt) or water (Control), and photographed 10 days after treatment. Bar = 1 cm. (B) Shoot chlorophyll contents of plants as indicated (salt treatment as in A), expressed as percentage of 0-day controls. Results shown are means \pm s.e. of three independent replicates. (C) Appearance of the fourth leaves of global and *sss1-1* plants grown under control conditions or 10 days after salt treatment. Plant growth and salinity treatments as described in Figure 1A. Bar = 1 cm. (D) Close-up images of leaves (as in A) stained with Trypan blue, revealing increased cell death in salt-treated *sss1-1* leaves. Bar = 0.5 mm.

***AtrbohF* confers salinity-induced ROS accumulation and soil-salinity tolerance**

Soil salinity causes ROS accumulation (Zhu, 2002; Munns and Tester, 2008; Miller *et al*, 2010; Mittler *et al*, 2011; Suzuki *et al*, 2011), and we have shown above that lack of *AtrbohF* (an NADPH oxidase enzyme catalysing ROS production) confers soil-salinity hypersensitivity (Figure 1A). We therefore next studied the relationship between *AtrbohF*-mediated ROS production and salinity tolerance. We first determined the effect of salinity on *in planta* ROS levels using nitroblue tetrazolium (NBT; in the presence of superoxide, NBT is reduced to a blue/purple formazan deposit; Carol *et al*, 2005). Salinity caused an increase in NBT staining in WT root stele cells (Figure 4A). Cross-sectional analysis revealed that this increase is localized primarily within pericycle and vascular parenchyma cells (Figure 4B), a cellular distribution pattern similar to that of *AtrbohF* transcripts (Figure 3H). In contrast, *atrbohF-F3* mutant roots did not display salinity-induced increases in stele-cell NBT staining or formazan deposits (Figure 4A–C). Thus, salinity induces the accumulation of NBT-detectable ROS in root stelar cells, and this accumulation is dependent on *AtrbohF* function.

We next showed that inhibition of NADPH oxidase activity with DPI (Carol *et al*, 2005) blocked salinity-induced NBT-detectable ROS accumulation in WT root stele (Figure 4D and E). We also found that DPI-treated WT plants phenocopied the soil-salinity hypersensitivity conferred by lack of *AtrbohF* (Figure 4F). We conclude that *AtrbohF* NADPH oxidase activity is necessary for salinity-induced ROS production and for consequent salinity tolerance.

Lack of *AtrbohF* function confers elevated shoot Na levels

Growth of plants on high-salinity soils causes excessive accumulation of Na ions in shoots and resultant cellular damage (due to toxicity and/or osmotic stress). We next determined if the soil-salinity hypersensitivity conferred by lack of *AtrbohF* function is due to increased shoot Na accumulation. We found that lack of *AtrbohF* function (*atrbohF-F3*; *sss1-1*) caused accumulation of >2-fold more shoot Na than in controls (global progenitor) during a 1- to 7-day period following watering with 120 mM NaCl (Figure 5A). Reduced shoot K content has been reported to cause Na accumulation in saline conditions, and Na accumulation can decrease K uptake (Zhu, 2002; Munns and Tester, 2008). We found that mutants lacking *AtrbohF* function showed K concentrations similar to WT 1–2 days following salinity treatment, and K concentrations marginally less than WT 4–7 days following treatment (Supplementary Figure 2A). Thus, lack of *AtrbohF* function confers increased shoot Na accumulation, an accumulation that is not obviously associated with a decrease in K content. The increased shoot Na accumulation caused by lack of *AtrbohF* function presumably explains the visible shoot soil-salinity hypersensitivity (bleaching and so on, Figure 1A) conferred by *AtrbohF* loss-of-function mutations.

We next determined the effects of DPI treatment on shoot accumulation of soil Na. Shoots of saline-soil-grown DPI-treated WT plants accumulated higher Na concentrations than controls (Figure 5B), suggesting that NADPH oxidase-generated ROS accumulation counters the accumulation of

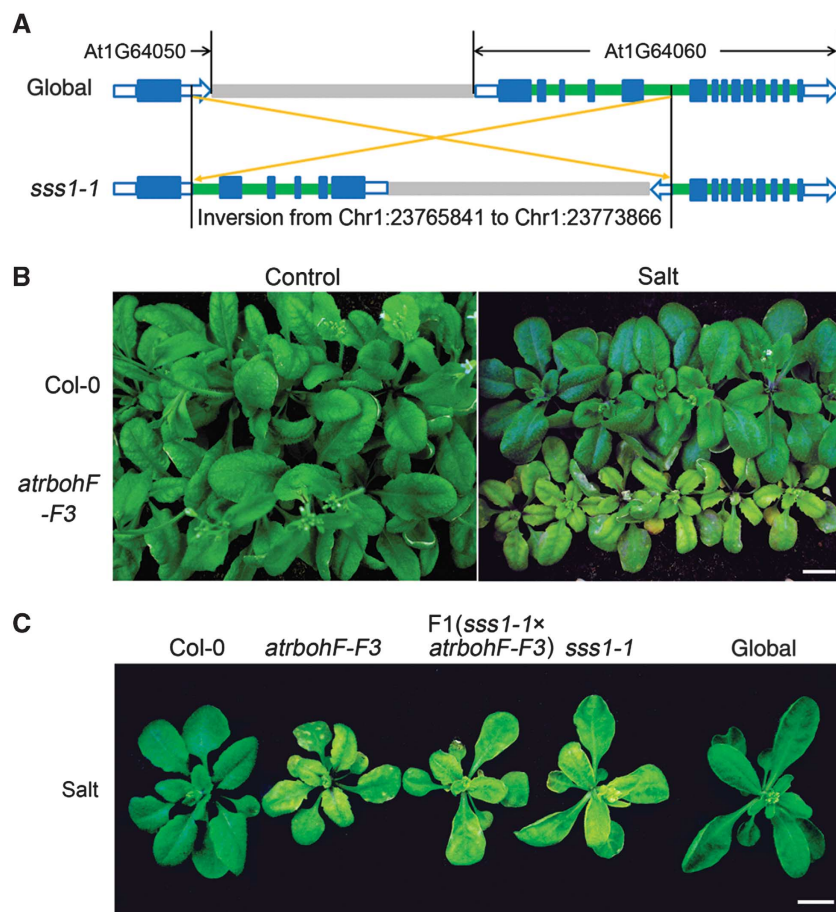


Figure 2 *sss1-1* is a novel mutant *AtrbohF* allele. (A) Cartoon showing the interstitial genomic inversion detected in *sss1-1* (versus global progenitor genome). The inversion interrupts *AtrbohF* (At1G64060). Blue boxes represent exons, green boxes introns, and grey boxes intergenic regions. Open blue boxes represent untranslated regions (UTR). (B) WT (Col-0) and *atrbohF-F3* plants grown in normal conditions (Control) or 7 days after salt treatment (Salt; salt treatment as in Figure 1A). Bar = 1 cm. (C) *sss1-1/atrbohF-F3* heterozygote and control homozygote plants (as indicated) 7 days after salt treatment. Plant growth and treatment is as in Figure 1A. Bar = 1 cm.

soil Na in untreated WT shoots. In contrast, DPI treatment of saline-soil-grown *atrbohF-F3* mutants caused only a marginal increase in their already elevated shoot Na concentrations (Figure 5B), suggesting that *AtrbohF* is the predominant NADPH oxidase countering shoot accumulation of soil Na. Consistent with this conclusion, lack of *AtrbohF* function (versus lack of function of alternative *Atrboh* genes) uniquely confers both soil-salinity hypersensitivity (Supplementary Figure 2B) and increased shoot Na accumulation (Supplementary Figure 2C). Thus, DPI treatment phenocopies both the salinity hypersensitivity (Figure 4F) and shoot Na accumulation phenotypes (Figure 5B) conferred by lack of *AtrbohF* function, indicating that ROS generated by *AtrbohF* has a specific and predominant role in regulating both Na accumulation and soil-salinity tolerance.

Lack of *AtrbohF* function confers elevation of xylem-sap Na concentration

Root-to-shoot delivery of soil Na is mediated by the xylem-based transpiration stream. *AtrbohF* has previously been reported to mediate stomatal closure induced by ethylene and ABA (Kwak *et al*, 2003; Desikan *et al*, 2006; Joshi-Saha *et al*, 2011). As stomatal aperture is a major determinant of

transpirational flow, we next determined if the increased shoot Na accumulation characteristic of *atrbohF-F3* mutants could be due to increased transpiration rate. However, while excess soil-salinity inhibited measured transpiration (Inan *et al*, 2004) of both WT and *atrbohF-F3* plants, there was no detectable difference between the transpiration rates of the two genotypes in either control or high soil-salinity conditions (Supplementary Figure 2D), suggesting that the elevated shoot Na accumulation of *atrbohF-F3* is unlikely to be due to effects on transpiration rate.

We next compared Na concentrations in the xylem sap of WT (Col-0) and *atrbohF-F3* plants by sampling root-pressure exudate from detopped plants. While the xylem-sap Na concentration of both WT and *atrbohF-F3* plants increased progressively over time following initiation of salt treatment, the *atrbohF-F3* xylem-sap Na concentration was consistently >2-fold higher than that of WT (Figure 5C; also see Materials and methods section). This elevated xylem-sap Na concentration presumably explains why the shoots of plants lacking *AtrbohF* function accumulate higher levels of Na than WT plants: increased xylem-sap Na concentrations, in combination with unaltered transpiration rates, will lead to increased delivery of soil Na from root to shoot (Smith, 1991).

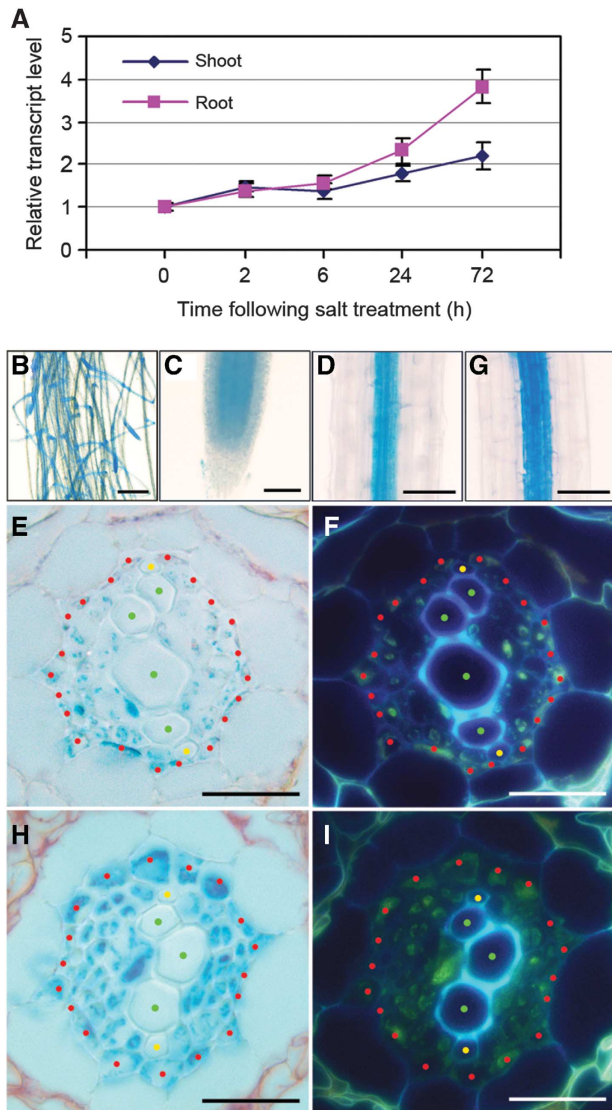


Figure 3 *AtrbohF* expression: cell/tissue specificity and salinity induction. (A) Real-time PCR analysis of salt-induced increase in *AtrbohF* transcript levels. Four-week-old hydroponically grown WT plants (see Materials and methods section) were treated with $\frac{1}{4}$ MS (control) or $\frac{1}{4}$ MS plus 100 mM NaCl. Samples were collected at times indicated. Data are expressed as fold increase of experimental samples over 0-h controls, and are means \pm s.e. of three replicates. (B–I) β -Glucuronidase staining of *pAtrbohF::GUS* plant tissues. (B) Root system; (C) root tip; (D, G) mature root; (E, H) cross-sections of mature root. (G, H) β -Glucuronidase staining of the mature root of *pAtrbohF::GUS* plants 3 days following salt (100 mM NaCl) treatment. (F, I) UV fluorescence images of root cross-sections shown in E and H. Bars = 1 cm in B; 100 μ m in C, D and G; 50 μ m in E, F, H and I. Locations of specific cell types are highlighted with red (pericycle), yellow (protoxylem) and green (metaxylem) dots in E, F, H, I; the tissue surrounding the xylem elements interior to the pericycle comprises vascular parenchyma and phloem cells. Results are from 4-week-old plants grown in hydroponic conditions (see Materials and methods section).

Lack of *AtrbohF* function confers rapid increase in stele cell Na⁺ levels

We next determined how lack of *AtrbohF* function causes increased xylem-sap Na concentrations by studying the accumulation and distribution of Na in root tissues of hydroponically cultured plants (see Materials and methods section).

Hydroponically cultured *atrbohF-F3* mutants displayed a salinity hypersensitivity phenotype similar to that observed when grown in soil (Supplementary Figure 2E), and likewise accumulated higher shoot Na levels than WT plants following onset of salinity treatment (Figure 5D). In addition, while *atrbohF-F3* root Na concentrations were higher than those of WT controls for the first 2 days following onset of hydroponic salt treatment (Figure 5E), *atrbohF-F3* and WT roots accumulated similar root Na concentrations following longer periods of exposure to salinity (days 4 and 7; Figure 5E).

We next visualized the specific sites of Na⁺ ion accumulation in roots exposed to salinity using CoroNa Green dye (a green-fluorescent indicator that increases emission intensity upon Na⁺ binding; Oh *et al*, 2009; Figure 5F–N). Fluorescence was barely detectable in cells of both WT and *atrbohF-F3* control roots (Figure 5F and G), but a strong fluorescence signal was detectable in diverse cell types following exposure to 100 mM NaCl (Figure 5H–N). In salt-treated WT roots, fluorescence was predominantly detected in epidermal cells (Figure 5H, K and M), and was faintly detectable in pericycle and vascular cells. In contrast, fluorescence became clearly detectable in both epidermal and pericycle cells of *atrbohF-F3* roots at 8 h after exposure onset (Figure 5I and J), with further increases in pericycle and vascular cells at 24 h (Figure 5L and O) and 96 h (Figure 5N and P). Thus, Na⁺ accumulates to higher than WT concentrations in the root vasculature of salinity-treated mutants lacking *AtrbohF* function, presumably explaining the elevated xylem-sap Na concentration characteristic of these mutants.

The saline-soil hypersensitivity of *atrbohF-F3* is transpiration dependent

To further understand the soil-salinity hypersensitivity conferred by lack of *AtrbohF* function, we next screened for novel mutations restoring normal soil-salinity tolerance to *atrbohF-F3* (see Materials and methods section). We thereby identified *repressor of soil-salinity sensitive 1-1* (*rss1-1*), a mutation suppressing the effects of *atrbohF-F3* on both visible soil-salinity hypersensitivity and chlorophyll levels in saline soils (Figure 6A and B). Whole-genome sequencing identified four novel mutations in the *rss1-1* genome (compared to the *atrbohF-F3* genome; Supplementary Figure 3A). Only one of the four novel mutations (the 2-bp deletion on Chr5 (–CA); Figure 6C) was uniformly homozygous in all salinity-tolerant F₂ plants. This deletion interrupts *A. thaliana cellulose synthesis catalytic subunit 7* (*AtCesa7*; Figure 6C).

To determine if loss of *AtCesa7* function was responsible for repressing the salt hypersensitivity of *atrbohF-F3* in *rss1-1*, we generated an independent line lacking *AtrbohF* and *AtCesa7* functions (*atrbohF-F3/AtCesa7^{irx3-4}*, Turner and Somerville, 1997), studied the salt sensitivity of this line compared to *atrbohF-F3*, and found that *atrbohF-F3/AtCesa7^{irx3-4}* displayed a salt tolerance phenotype (relative to *atrbohF-F3*) similar to that of *atrbohF-F3/AtCesa7^{rss3-4}* (Figure 6D). These observations indicated that *rss1-1* is a novel loss-of-function allele of *AtCesa7*.

Loss-of-function mutations of *AtCesa7* (e.g., *irregular xylem3* (*irx3*)) confer collapsed stem xylem (Turner and Somerville, 1997). Accordingly, our novel *AtCesa7^{rss1-1}* allele confers a marked reduction in the number of functional conducting root vasculature xylem elements

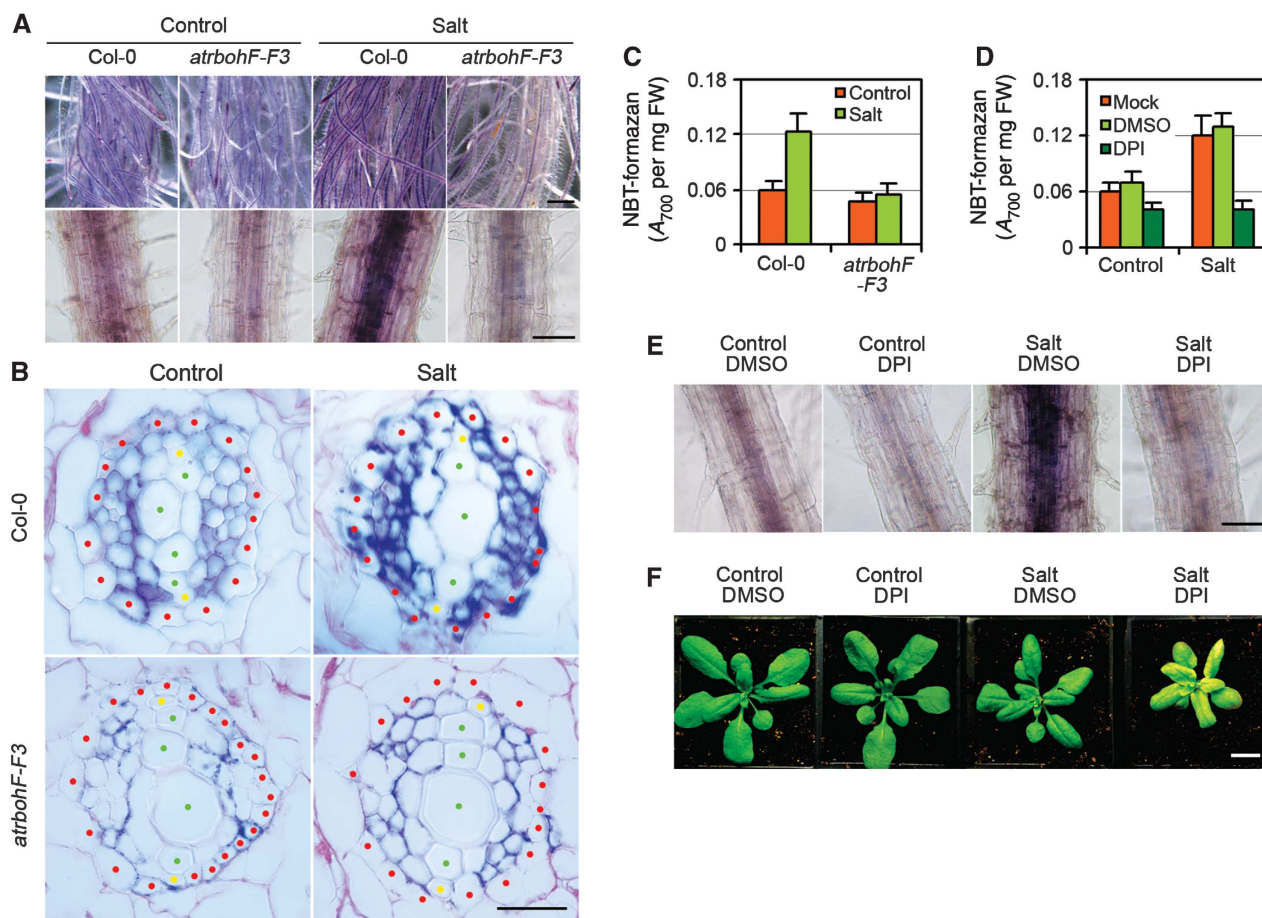


Figure 4 Soil-salinity tolerance conferred by *AtrbohF*-mediated ROS production in root vasculature. (A) Effect of salt on NBT-visualized ROS levels in WT (Col-0) and *atrbohF-F3* roots (see Materials and methods section). Upper panel shows strong NBT staining of the central stele area of salt-treated WT root systems, lower panel single root in close-up. Bar = 1 cm in upper panel; 100 μ m in lower panels. (B) Root cross-section (as in A). Locations of cell types are highlighted with red (pericycle), yellow (protoxylem) and green (metaxylem) dots; cells surrounding the xylem elements interior to the pericycle represent vascular parenchyma and phloem. Bars = 50 μ m. (C) Colorimetric quantification of NBT-formazan deposition in indicated root tissue (see Materials and methods section; FM, fresh mass). (D, E) DPI inhibits salt-induced NBT-formazan production in WT roots versus controls (DMSO is carrier; see Materials and methods section). Bar = 100 μ m. (F) WT (Col-0) plants 7 days following treatments (as indicated). Bar = 1 cm. Four-week-old plants were watered with either 120 mM NaCl (Salt) or water (Control), combined with 5 μ M of DPI or DPI carrier (DMSO), and photographed 7 days after treatment. Bar = 1 cm. Data shown in (C) and (D) are means \pm s.e. of three replicates.

(Supplementary Figure 3B). Loss of *AtCesA7* function has also been reported to confer reduced transpiration rate (Liang *et al*, 2010). Similarly, *AtCesA7^{rss1-1}* confers reduced transpiration rate versus WT and progenitor *atrbohF-F3* plants, and suppresses the transpiration of *atrbohF-F3* plants in both control and saline-soil growth conditions (Figure 7A and B). In addition, although shoot Na concentrations were relatively similar in *atrbohF-F3/AtCesA7^{rss1-1}* and *atrbohF-F3* plants grown in control conditions, *atrbohF-F3/AtCesA7^{rss1-1}* shoot Na levels were \sim 30% those of *atrbohF-F3* in saline soil (Figure 7C). As transpiration rate has a major effect on root-to-shoot Na delivery (Zhu, 2002; Møller and Tester, 2007; Munns and Tester, 2008), we conclude that *AtCesA7^{rss1-1}* suppresses the soil-salinity hypersensitivity of *atrbohF-F3* by reducing the transpiration rate and thus the transpiration-dependent root-to-shoot delivery of Na. This conclusion is strengthened by the observation that transpiration-restricting high atmospheric relative humidity (90%) reduces both the severity of the visible soil-salinity hypersensitivity phenotype and the

shoot Na accumulation of *atrbohF-F3* mutants grown on saline soil (Figure 7D–F).

Discussion

Plant roots supply soil mineral ions to shoots via the transpiration stream (Smith, 1991; Smith *et al*, 2010). Homeostatic regulation of shoot ion levels is necessary because many ions, such as Na, are toxic in excess. We here describe the discovery of a root-localized mechanism for regulation of root-to-shoot Na delivery. This mechanism contributes to shoot Na homeostasis and protects shoot cells from the damaging effects of excess Na accumulation. In essence, increased soil salinity triggers increased ROS production in root vasculature tissue. Local increases in ROS levels then cause reductions in root xylem-sap Na concentrations and in delivery of Na to the shoot in the transpiration stream.

Soil-salinity stress has long been known to cause the accumulation of ROS *in planta* (Miller *et al*, 2010; Mittler

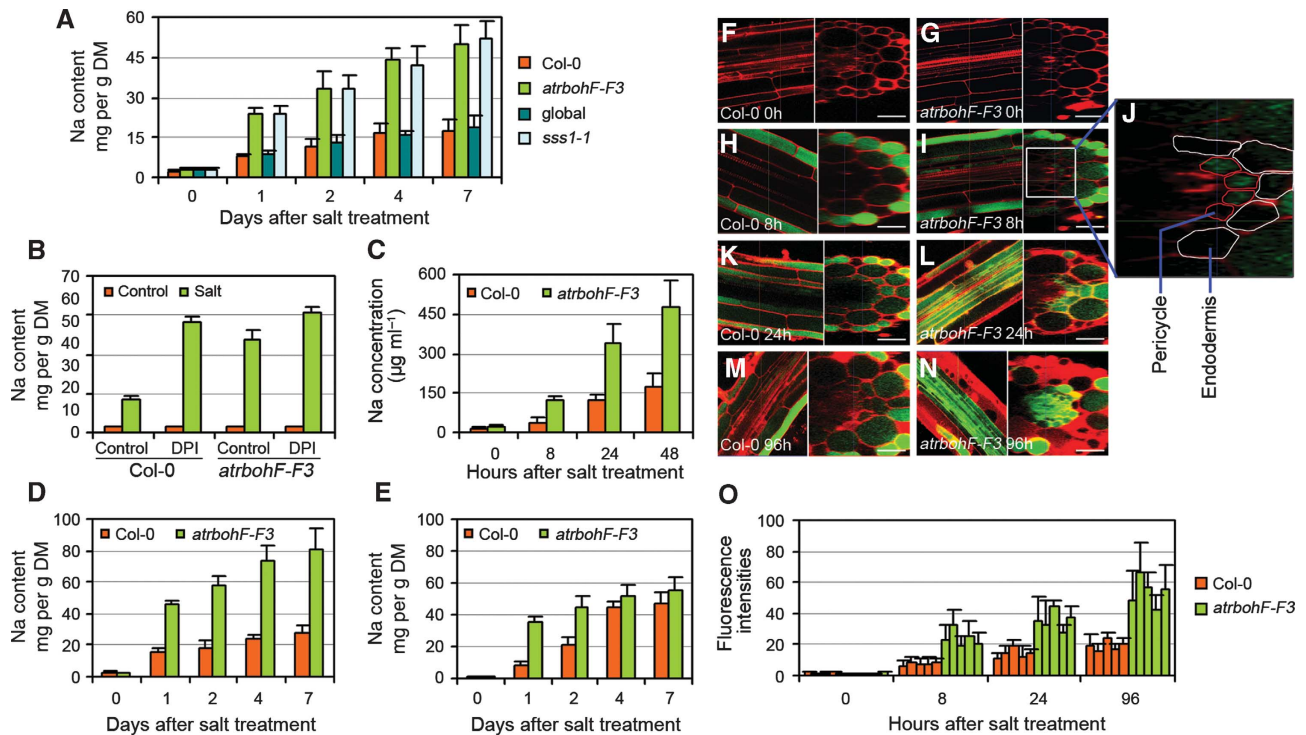


Figure 5 *AtrbohF*-mediated ROS regulation of root vasculature, xylem-sap and shoot Na levels. (A) Shoot Na contents (genotypes as indicated; global is control for *sss1-1*; Col-0 for *atrbohF-F3*; DM, dry mass) 0–7 days following salt treatment (as in Figure 1A). Na content determinations as in Materials and methods section. (B) Effect of DPI treatment on shoot Na content of WT versus *atrbohF-F3*. Salt and DPI treatment was as in Figure 4D. Shoot Na contents were determined 4 days following treatment. (C) Xylem-sap Na concentrations, measured in root-pressure exudate collected from detopped plants, following salt treatment of soil-grown WT (Col-0) and *atrbohF-F3* (see Materials and methods section). (D, E) Shoot (D) and root (E) Na content of hydroponically grown WT (Col-0) and *atrbohF-F3* 0–7 days following salt treatment. Plant growth and salt treatments as in Figure 2A. Data shown in A–E are means \pm s.e. of three replicates. (F–N) Cellular localization of Na⁺ in salt-treated WT and *atrbohF-F3* roots. Confocal images of roots stained with CoroNa Green (green) and propidium iodide (red) are shown. (F, G) WT (Col-0; F) and *atrbohF-F3* (G) roots without salt treatment; left panel longitudinal section, right panel transverse section. (H–N) Cellular localization of Na⁺ in WT (H, K, M) and *atrbohF-F3* (I, J, L, N) roots following 8 h (H–J), 24 h (K, L) and 96 h (M, N) of salt treatment. Salt treatment as in Figure 2A. Bar = 50 μ m. (O) Quantitative comparison of CoroNa Green fluorescence intensities in root pericycle cells. Five individual plants were measured for each genotype. Values are means \pm s.e. for 20 pericycle cells from each individual plant.

et al, 2011). ROS is toxic and causes oxidative stress and cell damage (Miller *et al*, 2010; Mittler *et al*, 2011; Suzuki *et al*, 2011), but is also a potential response signalling mediator (Miller *et al*, 2007, 2010; Achard *et al*, 2008; Kaye *et al*, 2011; Mittler *et al*, 2011; Suzuki *et al*, 2011; Ma *et al*, 2012). We have discovered a cellular signalling mechanism via which soil-salinity-induced ROS regulates shoot Na homeostasis. This discovery rests on our initial observation that *AtrbohF* (a gene encoding an important NADPH oxidase regulator of ROS production; Sagi and Fluhr, 2006) confers tolerance of high soil salinity (Figures 1–3). Multiple distinct NADPH oxidases are encoded by the *Arabidopsis* genome (by genes *AtrbohA*–*AtrbohJ*; Sagi and Fluhr, 2006). Previous reports have associated lack of *AtrbohJ* or *AtrbohD* function with *in vitro* salt hypersensitivity (*atrbohJ*; Kaye *et al*, 2011) or *in vitro* salt tolerance (*atrbohD*; Xie *et al*, 2011; Ma *et al*, 2012; Marino *et al*, 2012), and further studies suggest that *AtrbohF* acts redundantly with *AtrbohD* in regulating *in vitro* salt responses (Xie *et al*, 2011; Ma *et al*, 2012). However, these previous and our own studies have shown that lack of *AtrbohF* function alone had no detectable effect on *in vitro* salt sensitivity (Supplementary Figure 1C; Xie *et al*, 2011; Ma *et al*, 2012). In marked contrast, we find that lack of *AtrbohF* function alone confers severe soil-salinity hypersensitivity,

and that *AtrbohF* is predominant among NADPH oxidase-encoding loci in the control of soil-salinity tolerance (Supplementary Figure 2B). As transpiration is negligible in *in vitro* grown plants, we propose that *AtrbohF* specifically conditions the transpiration-dependent aspects of soil-salinity tolerance. This proposal is strengthened by our observation that a decrease in transpiration rate, either via genetic mutation (e.g., *AtCesa7^{rss1-1}*; Figure 6A) or via an increase in atmospheric relative humidity (Figure 7D–F), suppresses the soil-salinity hypersensitivity of *atrbohF-F3*. We conclude that *AtrbohF* specifically regulates transpiration-dependent soil-salinity response and tolerance.

When plants are grown under Na stress conditions, the accumulation of shoot Na⁺ ions leads to cellular injury (arising from metabolic toxicity and/or osmotic stress; Zhu, 2002; Munns and Tester, 2008). A previous report indicates that mutants lacking *AtrbohF* function accumulate similar to WT levels of Na when grown on high salt *in vitro* (Ma *et al*, 2012). In contrast, our experiments have shown that *AtrbohF*-dependent accumulation of ROS in root vasculature actually plays an important role in regulation of vascular Na concentration and consequent shoot Na concentration (Figure 5). This difference is again attributable to large differences in transpiration rates in the two experimental

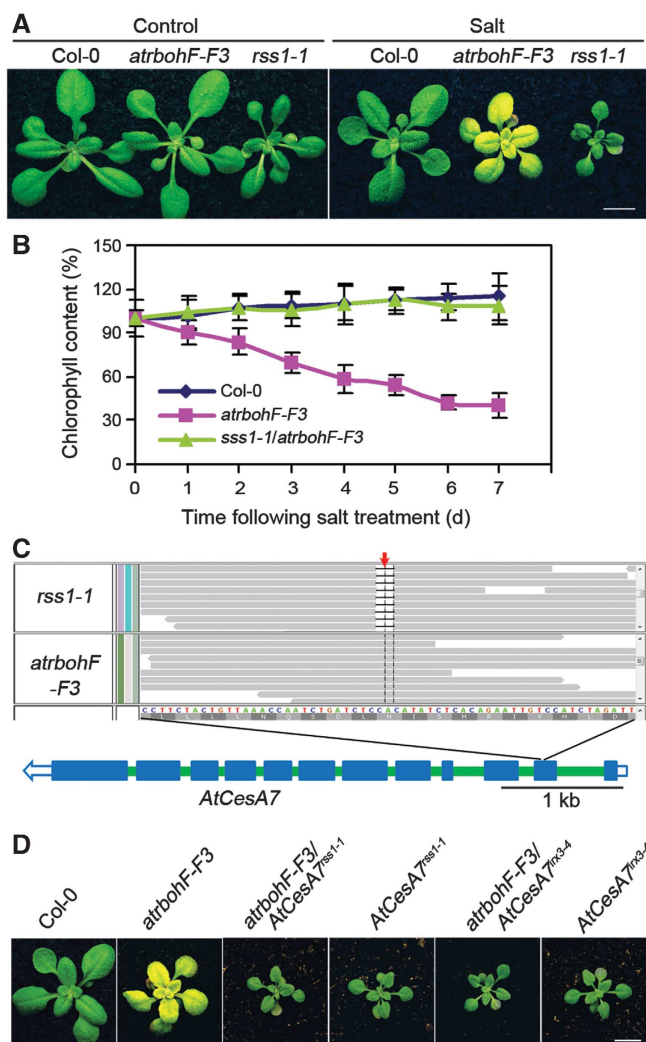


Figure 6 *rss1-1* is a novel mutant *AtCesA7* allele. (A) Soil-grown plants (genotypes as indicated) grown under control conditions (Control) and 7 days after salt treatment (Salt). Bar = 1 cm. (B) Chlorophyll content of soil-grown plants. Genotypes as indicated (salt treatments were as described in Figure 1A). (C) The mutation causing *rss1-1* phenotype. The top panel shows the 2-bp deletion (-CA; highlighted by the red arrow) that interrupts *AtCesA7* in *rss1-1*. Reads from *rss1-1* and *atrbohF-F3* are aligned against TAIR9. The bottom panel shows the genomic structure of *AtCesA7*. Blue boxes represent coding sequence, green boxes introns, open blue boxes untranslated regions (UTR). (D) Demonstration that *rss1-1* is a mutant *AtCesA7* allele. *atrbohF-F3/AtCesA7^{rss3-4}* is less sensitive to soil salinity compared to *atrbohF-F3* and shows a salt sensitivity similar to that of *atrbohF-F3/AtCesA7^{rss1-1}*. Bar = 1 cm.

systems (Figure 7). Our observations indicate that, when the transpiration stream is functioning, and under high-salinity conditions, loss of *AtrbohF* function increases root vasculature Na levels (Figure 5F–N), increases xylem-sap Na concentration (Figure 5C), and in consequence increases delivery of Na to the shoot, resulting in elevated shoot Na accumulation (Figure 5A). This elevated accumulation of Na in the shoot causes the visible damage associated with soil-salinity hypersensitivity.

A previous report has shown that salinity tolerance can be increased by engineered expression of *HKT1* in root stele (Møller *et al*, 2009), indicating that stele-specific regulation of Na concentration underlies salinity tolerance. In addition, while previous reports have suggested that salinity stress induces stele-specific ROS (Dinneny *et al*, 2008; Dinneny, 2010), the mechanism and biological significance of this induction remained poorly understood. We here show that salinity-induced ROS accumulation in the root stele

is substantially attributable to *AtrbohF* function (Figure 4A–C), and that *AtrbohF*-dependent accumulation of ROS in the stele confers regulation of shoot Na delivery and tolerance. We propose that, in WT root vasculature, localized salt-induced increases in *AtrbohF* transcript levels (Figure 3A; and also possible post-translational activation of *AtrbohF* (Sirichandra *et al*, 2009; Yun *et al*, 2011) cause an increase in *AtrbohF* activity, thereby increasing local ROS levels (Figure 4A–C). The resultant elevated vascular ROS then inhibits net accumulation of Na in the xylem sap and transpiration stream (Figure 5C and F–O), thus protecting cells of the shoot from the elevated Na⁺ that would otherwise be delivered to them. There is considerable experimental evidence that elevated ROS cause increased cytosolic free Ca²⁺ concentrations (Foreman *et al*, 2003), and that these in turn can lead to improved cellular K/Na homeostasis by enhancing Na⁺ extrusion and maintaining K⁺ influx (Demidchik *et al*, 2002; Zhu, 2002; Munns and Tester,

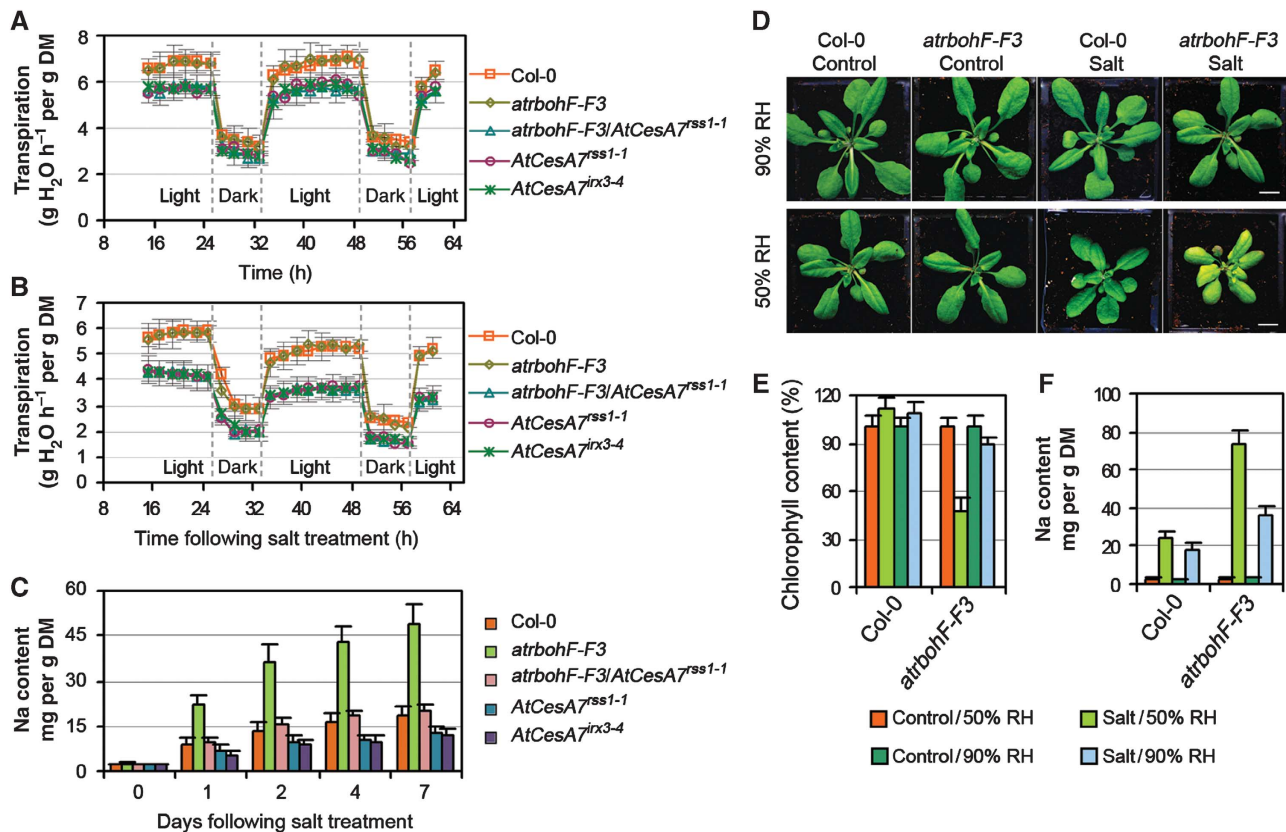


Figure 7 The soil-salinity hypersensitivity of *atrbohF-F3* is transpiration-dependent. (A, B) Comparison of transpiration rate of plants (genotypes as indicated) under control conditions (A) or following salt treatment (B) over the experimental period (see Materials and methods section). Values are means \pm s.e. of at least eight plants. (C) Shoot Na content of plants (genotypes as indicated) 0–7 days following salt treatment (salt treatment as described in Figure 1A). Values are means \pm s.e. for three replicates. (D–F) The *atrbohF-F3* plant displays a mild salt hypersensitivity when grown at 90% relative humidity (RH); versus when grown at 50% RH). Appearance (D), chlorophyll content (E) and shoot Na concentration (F) of Col-0 and *atrbohF-F3* plants grown in conditions as indicated. Data are means \pm s.e. of two replicates.

2008). A speculative possibility is that increased ROS might stimulate the activity of HKT transporters in the vasculature, which are known to be important in controlling xylem-sap Na levels and the consequential salt load on the shoot.

In summary, we have discovered a novel salinity-activated, ROS-regulated, root-localized control on root–shoot Na transport via the transpiration stream. This control contributes to essential shoot ionic homeostasis in transpiring plants and identifies a potential target for increasing the salinity tolerance of a wide range of agricultural crop species.

Materials and methods

Plant materials

The DELLA-deficient (*gai-t6*, *rga-t2*, *rgl1-1*, *rgl2-1* and *rgl3-4*; global) progenitor, *atrbohF-F3*, *atrbohD* and *atrbohF-F3/atrbohD* mutants were as previously described (Torres *et al*, 2002; Belfield *et al*, 2012). *atrbohI* (N53622), *atrbohJ*, *atrbohH* (SALK_558170), *atrbohE* (SALK_564850), *atrbohC* (SALK_058191) and *AtCesA^{irx3-4}* (SALK_029940C) mutant lines were obtained from the European *Arabidopsis* Stock Centre (<http://Arabidopsis.info>).

Soil and hydroponic *Arabidopsis* culture

Soil: Seeds were sown on Erin Multipurpose compost (Erin Horticulture; <http://www.erinhorticulture.com>) and grown in controlled environments (16/8-h light/dark cycle, 22°C, 50–60% relative humidity). **Hydroponics:** Sterilized seeds were sown on sponges (approximately 1 cm thick) saturated with $\frac{1}{4}$ MS solution. The seeds

were first stratified at 4 °C for 3 days in the dark. Subsequently, the sponges were suspended over $\frac{1}{4}$ MS solution. Plants were grown in controlled environments as described above, and the $\frac{1}{4}$ MS solution was replaced with new media twice a week.

Mutant screen

Fast neutron-mutagenised M₂ global seeds (Belfield *et al*, 2012) were sown on Erin Multipurpose compost, grown for 4 weeks (conditions as above), then watered once to soil saturation with 120 mM NaCl solution. After 5 days, all plants displaying salinity hypersensitive phenotypes (bleached or pale leaves) were transferred to normal soil and grown to seed set. To screen for *atrbohF-F3* suppressors, *atrbohF-F3* seeds were fast neutron mutagenised as in Belfield *et al* (2012). M₂ descendants were screened as above, but salt-tolerant individuals (relative to *atrbohF-F3*) were collected.

Salt treatment under agar plate conditions

Seven-day-old plants grown on MS agar plates (1% (w/v) sucrose); 16/8-h light/dark cycle, 22°C) were transferred to MS agar plates (1% (w/v) sucrose) with a range of NaCl concentrations.

Illumina sequencing and detection of mutations

Genomic re-sequencing of *sss1-1* and *rss1-1* mutants was performed at the Beijing Genomics Institute, China (using the Illumina Genome Analyzer II platform). We followed previous protocols (Jiang *et al*, 2011) to detect novel mutations versus progenitor reference genomes (*sss1-1* versus the global-reference sequence (Belfield *et al*, 2012) and *rss1-1* versus *atrbohF-F3*).

Transcription analyses

Real-time PCR was performed as previously described (Jiang *et al*, 2007). Primer pairs used for PCR amplification of each gene were as follows: *AtrbohF*: 5' rCAGCATTGAGCCAAAACCT-3' and 5anTG CTCCTTTGGCTGTGAGTA-3'; *CBP20*: 5' PGAAGGAAGACAATGG GGCCG-3' and 5anCGGCCATAGCGATCATCGTC-3'.

Constructs and plant transformation

Approximately 2.3 kb DNA upstream of *AtrbohF* was amplified from Col-0 genomic DNA using the following primers: *AtrbohF* PF, 5'PFGGGGACAAGTTTGTACAAAAAAGCAGGCTTCCCCAGTTATGTGT GCATGT-3', and *AtrbohF* PR, 5'PRGGGGACCACCTTGTACAAGAAAG CTGGGTCCAGATCCAAAGTCGGAATTC-3'. This fragment was cloned into pMDC163 using Gateway Technology (Invitrogen) to generate the *pAtrbohF-GUS* construct, which was then introduced into *Agrobacterium tumefaciens* strain GV3101 and transformed into the Col-0 laboratory strain.

Chlorophyll determination

We determined the chlorophyll content as previously described (Jiang *et al*, 2007).

Cell-death staining and GUS staining

We stained dead cells with Trypan blue as previously described (Carol *et al*, 2005), and performed GUS staining as described in Jiang *et al* (2007).

Determination of ROS accumulation

NBT staining and formazan deposit qualification were as previously described (Carol *et al*, 2005; Myouga *et al*, 2008).

Determination of transpiration rate

We determined the transpiration rate as previously described (Inan *et al*, 2004). In brief, 4-week-old plants grown singly in 4-cm pots were watered to soil capacity with water or 120 mM NaCl solution. Pots were then sealed with plastic wrap, leaving shoots outside the wrap (to avoid water loss from soil surface and bottom of the pots), and weighed on an electronic balance every 2 h for 2 days (measurements began 12 h after treatments) to measure transpiration rate.

Determination of ion content

Plant material was harvested, oven dried for at least 24 h at 80 °C and weighed. The material was then digested in concentrated (69%, v/v) HNO₃ for at least 12 h for elemental extraction. Concentrations of Na and potassium were determined in appropriately diluted samples by atomic absorption spectrophotometry in an air-acetylene flame (AAAnalysis100: Perkin-Elmer; <http://www.perkinelmer.com>).

References

Achard P, Cheng H, De Grauwe L, Decat J, Schoutteten H, Moritz T, Van Der Straeten D, Peng J, Harberd NP (2006) Integration of plant responses to environmentally activated phytohormonal signals. *Science* **311**: 91–94

Achard P, Renou JP, Berthomé R, Harberd NP, Genschik P (2008) Plant DELLAs restrain growth and promote survival of adversity by reducing the levels of reactive oxygen species. *Curr Biol* **18**: 656–660

Amtmann A, Sanders D (1999) Mechanisms of Na⁺ uptake by plant cells. *Adv Bot Res* **29**: 75–112

Baxter I, Brazelton JN, Yu D, Huang Y, Lahner B, Nordborg M, Vitek O, Salt DE (2010) A coastal cline in sodium accumulation in *Arabidopsis thaliana* is driven by natural variation of the sodium transporter AtHKT1;1. *PLoS Genet* **6**: e1001193

Belfield EJ, Gan X, Mithani A, Brown C, Jiang C, Franklin K, Alvey E, Wibowo A, Jung M, Bailey K, Kalwani S, Ragoussis J, Mott R, Harberd NP (2012) Genome-wide analysis of mutations in mutant lineages selected following fast-neutron irradiation mutagenesis of *Arabidopsis thaliana*. *Genome Res* **22**: 1306–1315

Measurement of xylem-sap Na concentration

Five-week-old plants were used for measurement of xylem-sap Na concentration. To collect samples of xylem sap, the rosette leaves and inflorescence stems were excised at the base of the main stem axis. Plants were then kept in a chamber at >95% relative humidity. Sap exuding at the cut surface of the detopped root system was collected and pooled from approximately 20 replicate individual plants. Five microlitres of xylem sap was added to 45 µl of concentrated (69%, v/v) HNO₃, incubated for at least 12 h, and then diluted to 5 ml with water for ion content measurement.

Visualization of cellular Na⁺ concentration

Four-week-old hydroponically grown seedlings were stained and observed by confocal microscopy (Zeiss LSM 510) after salinity treatment. Staining for Na⁺ was performed as described by Oh *et al* (2009).

Visualization of xylem

To visualize root xylem cells (Supplementary Figure 3B), we stained transverse root sections (8 µm thick) from 4-week-old plants with toluidine blue.

Supplementary data

Supplementary data are available at *The EMBO Journal* Online (<http://www.embojournal.org>).

Acknowledgements

We thank Liam Dolan for *atrbohI*, *atrbohJ*, *atrbohH*, *atrbohE* and *atrbohC* seeds, Jian-Kang Zhu and Yan Guo for stimulating discussion, and Xiangchao Gan for assistance with genome sequence analysis. This publication is based on the work supported by Award No. KUK-I1-002-03, made by King Abdullah University of Science and Technology, and by Biotechnology and Biological Sciences Research Council (BBSRC) grants BB/F020759/1 and BB/F022697/1. RM and JR are supported by the Wellcome Trust grant 075491/Z/04.

Author contributions: CJ, EB, AV, JACS and NPH conceived the study and wrote the paper. CJ carried out the mutant screens. CJ, AM, JR and RM analysed the genome sequencing data. CJ generated the *pAtrbohF:GUS* and *35S:AtrbohF/atrbohF-F3* transgenic lines and implemented genetic crosses between mutants. CJ and JACS measured the ion contents. CJ carried out studies of NBT staining, GUS staining, Trypan blue staining, CoroNa staining, chlorophyll measurement and DPI treatment.

Conflict of interest

The authors declare that they have no conflict of interest.

Carol RJ, Takeda S, Linstead P, Durrant MC, Kakesova H, Derbyshire P, Drea S, Zarsky V, Dolan L (2005) A RhoGDP dissociation inhibitor spatially regulates growth in root hair cells. *Nature* **438**: 1013–1016

Dat J, Vandenabeele S, Vranová E, Van Montagu M, Inzé D, Van Breusegem F (2000) Dual action of the active oxygen species during plant stress responses. *Cell Mol Life Sci* **57**: 779–795

Davenport RJ, Muñoz-Mayor A, Jha D, Essah PA, Rus A, Tester M (2007) The Na⁺ transporter AtHKT1 controls xylem retrieval of Na⁺ in *Arabidopsis*. *Plant Cell Environ* **30**: 497–507

Demidchik V, Davenport RJ, Tester M (2002) Nonselective cation channels in plants. *Annu Rev Plant Biol* **53**: 67–107

Desikan R, Last K, Harrett-Williams R, Tagliavia C, Harter K, Hooley R, Hancock JT, Neill SJ (2006) Ethylene-induced stomatal closure in *Arabidopsis* occurs via AtrbohF-mediated hydrogen peroxide synthesis. *Plant J* **147**: 907–916

Dinneny JR (2010) Analysis of the salt-stress response at cell-type resolution. *Plant Cell Environ* **33**: 543–551

Dinneny JR, Long TA, Wang JY, Jung JW, Mace D, Pointer S, Barron C, Brady SM, Schiefelbein J, Benfey PN (2008) Cell identity

- mediates the response of *Arabidopsis* roots to abiotic stress. *Science* **320**: 942–945
- Epstein E (1985) Salt-tolerant crops: origins, development, and prospects of the concept. *Plant Soil* **89**: 187–198
- Flowers TJ (2004) Improving crop salt tolerance. *J Exp Bot* **55**: 307–319
- Frommer WB, Ludewig U, Rentsch D (1999) Taking transgenic plants with a pinch of salt. *Science* **285**: 1222–1223
- Foreman J, Demidchik V, Bothwell JH, Mylona P, Miedema H, Torres MA, Linstead P, Costa S, Brownlee C, Jones JD, Davies JM, Dolan L (2003) Reactive oxygen species produced by NADPH oxidase regulate plant cell growth. *Nature* **422**: 442–446
- Greenway H, Munns RA (1980) Mechanisms of salt tolerance in non-halophytes. *Annu Rev Plant Physiol* **31**: 149–190
- Inan G, Zhang Q, Li P, Wang Z, Cao Z, Zhang H, Zhang C, Quist TM, Goodwin SM, Zhu J, Shi H, Damsz B, Charbaji T, Gong Q, Ma S, Fredricksen M, Galbraith DW, Jenks MA, Rhodes D, Hasegawa PM *et al.* (2004) Salt cress. A halophyte and cryophyte *Arabidopsis* relative model system and its applicability to molecular genetic analyses of growth and development of extremophiles. *Plant Physiol* **135**: 1718–1737
- Jiang C, Gao X, Liao L, Harberd NP, Fu X (2007) Phosphate starvation root architecture and anthocyanin accumulation responses are modulated by the gibberellin-DELLA signaling pathway in *Arabidopsis*. *Plant Physiol* **145**: 1460–1470
- Jiang C, Mithani A, Gan X, Belfield EJ, Klingler JP, Zhu J-K, Ragoussis J, Mott R, Harberd NP (2011) Regenerant *Arabidopsis* lineages display a distinct genome-wide spectrum of mutations conferring variant phenotypes. *Curr Biol* **21**: 1385–1390
- Joshi-Saha A, Valon C, Leung J (2011) Brand new START: abscisic acid perception and transduction in the guard cell. *Sci Signal* **4**: 1–13
- Kaye Y, Golani Y, Singer Y, Leshem Y, Cohen G, Ercetin M, Gillaspay G, Levine A (2011) Inositol polyphosphate 5-phosphatase7 regulates the production of reactive oxygen species and salt tolerance in *Arabidopsis*. *Plant Physiol* **157**: 229–241
- Kwak JM, Mori IC, Pei ZM, Leonhardt N, Torres MA, Dangl JL, Bloom RE, Bodde S, Jones JD, Schroeder JI (2003) NADPH oxidase *AtrbohD* and *AtrbohF* genes function in ROS-dependent ABA signaling in *Arabidopsis*. *EMBO J* **22**: 2623–2633
- Leshem Y, Seri L, Levine A (2007) Induction of phosphatidylinositol 3-kinase-mediated endocytosis by salt stress leads to intracellular production of reactive oxygen species and salt tolerance. *Plant J* **51**: 185–197
- Liang Y-K, Xie X, Lindsay SE, Wang YB, Masle J, Williamson L, Leyser O, Hetherington AM (2010) Cell wall composition contributes to the control of transpiration efficiency in *Arabidopsis thaliana*. *Plant J* **64**: 679–686
- Liu J, Ishitani M, Halfter U, Kim C-S, Zhu J-K (2000) The *Arabidopsis thaliana* *SOS2* gene encodes a protein kinase that is required for salt tolerance. *Proc Natl Acad Sci USA* **97**: 3730–3734
- Ma L, Zhang H, Sun L, Jiao Y, Zhang G, Miao C, Hao F (2012) NADPH oxidase *AtrbohD* and *AtrbohF* function in ROS-dependent regulation of Na^+/K^+ homeostasis in *Arabidopsis* under salt stress. *J Exp Bot* **63**: 305–317
- Marino D, Dunand C, Puppo A, Pauly N (2012) A burst of plant NADPH oxidases. *Trends Plant Sci* **17**: 9–15
- Mäser P, Eckelman B, Vaidyanathan R, Horie T, Fairbairn DJ, Kubo M, Yamagami M, Yamaguchi K, Nishimura M, Uozumi N, Robertson W, Sussman MR, Schroeder JI (2002) Altered shoot/root Na^+ distribution and bifurcating salt sensitivity in *Arabidopsis* by genetic disruption of the Na^+ transporter *AtHKT1*. *FEBS Lett* **531**: 157–161
- Miller G, Suzuki N, Ciftci-Yilmaz S, Mittler R (2010) Reactive oxygen species homeostasis and signalling during drought and salinity stresses. *Plant Cell Environ* **33**: 453–467
- Miller G, Suzuki N, Rizhsky L, Hegie A, Koussevitzky S, Mittler R (2007) Double mutants deficient in cytosolic and thylakoid ascorbate peroxidase reveal a complex mode of interaction between reactive oxygen species, plant development, and a response to abiotic stress. *Plant Physiol* **144**: 1777–1785
- Mittler R, Vanderauwera S, Suzuki N, Miller G, Tognetti VB, Vandepoele K, Gollery M, Shulaev V, Breusegem FV (2011) ROS signaling: the new wave? *Trends Plant Sci* **16**: 300–309
- Møller IS, Gilliam M, Jha D, Mayo GM, Roy SJ, Coates JC, Haseloff J, Tester M (2009) Shoot Na^+ exclusion and increased salinity tolerance engineered by cell type-specific alteration of Na^+ transport in *Arabidopsis*. *Plant Cell* **21**: 2163–2178
- Møller IS, Tester M (2007) Salinity tolerance of *Arabidopsis*: a good model for cereals? *Trends Plant Sci* **12**: 534–540
- Munns R, James RA, Xu B, Athman A, Conn SJ, Jordans C, Byrt CS, Hare RA, Tyerman SD, Tester M, Plett D, Gilliam M (2012) Wheat grain yield on saline soils is improved by an ancestral Na^+ transporter gene. *Nature Biotech* **30**: 360–364
- Munns R, Tester M (2008) Mechanisms of salinity tolerance. *Annu Rev Plant Biol* **59**: 651–681
- Myouga F, Hosoda C, Umezawa T, Iizumi H, Kuromori T, Motohashi R, Shono Y, Nagata N, Ikeuchi M, Shinozaki K (2008) A heterocomplex of iron superoxide dismutases defends chloroplast nucleoids against oxidative stress and is essential for chloroplast development in *Arabidopsis*. *Plant Cell* **20**: 3148–3162
- Oh DH, Leidi E, Zhang Q, Hwang SM, Li Y, Quintero FJ, Jiang X, D'Urzo MP, Lee SY, Zhao Y, Bahk JD, Bressan RA, Yun DJ, Pardo JM, Bohnert HJ (2009) Loss of halophytism by interference with *SOS1* expression. *Plant Physiol* **151**: 210–222
- Qiu QS, Guo Y, Dietrich MA, Schumaker KS, Zhu JK (2002) Regulation of *SOS1*, a plasma membrane Na^+/H^+ exchanger in *Arabidopsis thaliana*, by *SOS2* and *SOS3*. *Proc Natl Acad Sci USA* **99**: 8436–8441
- Qiu QS, Guo Y, Quintero FJ, Pardo JM, Schumaker KS, Zhu JK (2004) Regulation of vacuolar Na^+/H^+ exchange in *Arabidopsis thaliana* by the salt-overly-sensitive (*SOS*) pathway. *J Biol Chem* **279**: 207–215
- Quan R, Lin H, Mendoza I, Zhang Y, Cao W, Yang Y, Shang M, Chen S, Pardo JM, Guo Y (2007) *SCABP8/CBL10*, a putative calcium sensor, interacts with the protein kinase *SOS2* to protect *Arabidopsis* shoots from salt stress. *Plant Cell* **9**: 1415–1431
- Quesada V, Ponce MR, Micol JL (2000) Genetic analysis of salt-tolerant mutants in *Arabidopsis thaliana*. *Genetics* **154**: 421–436
- Quintero FJ, Martinez-Atienza J, Villalta I, Jiang X, Kim WY, Ali Z, Fujii H, Mendoza I, Yun DJ, Zhu JK, Pardo JM (2011) Activation of the plasma membrane Na/H antiporter salt-overly-sensitive 1 (*SOS1*) by phosphorylation of an auto-inhibitory C-terminal domain. *Proc Natl Acad Sci USA* **108**: 2611–2616
- Ren ZH, Gao JP, Li LG, Cai XL, Huang W, Chao DY, Zhu MZ, Wang ZY, Luan S, Lin HX (2005) A rice quantitative trait locus for salt tolerance encodes a sodium transporter. *Nat Genet* **37**: 1141–1146
- Sagi M, Fluhr R (2006) Production of reactive oxygen species by plant NADPH oxidases. *Plant Physiol* **141**: 336–340
- Shi H, Quintero FJ, Pardo JM, Zhu J-K (2002) The putative plasma membrane Na^+/H^+ antiporter *SOS1* controls long-distance Na^+ transport in plants. *Plant Cell* **14**: 465–477
- Sirichandra C, Gu D, Hu HC, Davanture M, Lee S, Djaoui M, Valot B, Zivy M, Leung J, Merlot S, Kwak JM (2009) Phosphorylation of the *Arabidopsis* *AtrbohF* NADPH oxidase by *OST1* protein kinase. *FEBS Lett* **583**: 2982–2986
- Smith AM, Coupland G, Dolan L, Harberd N, Jones J, Martin C, Sablowski R, Amey A (2010) *Plant Biology*. New York, USA: Garland Science, Taylor & Francis Group, LLC
- Smith JAC (1991) Ion transport and the transpiration stream. *Bot Acta* **104**: 416–421
- Sunardi Horie T, Motoda J, Kubo M, Yang H, Yoda K, Horie R, Chan WY, Leung HY, Hattori K, Konomi M, Osumi M, Yamagami M, Schroeder JI, Uozumi N (2005) Enhanced salt tolerance mediated by *AtHKT1* transporter-induced Na unloading from xylem vessels to xylem parenchyma cells. *Plant J* **44**: 928–938
- Suzuki N, Miller G, Morales J, Shulaev V, Torres MA, Mittler R (2011) Respiratory burst oxidases: the engines of ROS signalling. *Curr Opin Plant Biol* **14**: 691–699
- Tester M, Davenport RJ (2003) Na^+ transport and Na^+ tolerance in higher plants. *Ann Bot* **91**: 503–527
- Torres MA, Dangl JL, Jones JG (2002) *Arabidopsis* *gp91phox* homologues *AtrbohD* and *AtrbohF* are required for accumulation of reactive oxygen intermediates in the plant defence response. *Proc Natl Acad Sci USA* **99**: 517–522

- Torres MA, Jones JD, Dangi JL (2005) Pathogen-induced, NADPH oxidase-derived reactive oxygen intermediates suppress spread of cell death in *Arabidopsis thaliana*. *Nat Genet* **37**: 1130–1134
- Turner SR, Somerville CR (1997) Collapsed xylem phenotype of *Arabidopsis* identifies mutants deficient in cellulose deposition in the secondary cell wall. *Plant Cell* **9**: 689–701
- Xie YJ, Xu S, Han B, Wu MZ, Yuan XX, Han Y, Gu Q, Xu DK, Yang Q, Shen WB (2011) Evidence of *Arabidopsis* salt acclimation induced by up-regulation of HY1 and the regulatory role of RbohD-derived reactive oxygen species synthesis. *Plant J* **66**: 280–292
- Yun BW, Feechan A, Yin M, Saidi NB, Le Bihan T, Yu M, Moore JW, Kang JG, Kwon E, Spoel SH, Pallas JA, Loake GJ (2011) S-nitrosylation of NADPH oxidase regulates cell death in plant immunity. *Nature* **478**: 264–268
- Zhu J-K (2002) Salt and drought stress signal transduction in plants. *Annu Rev Plant Biol* **53**: 247–273